Agro-Industrial Waste Valorization for Enhanced Acetoin Production through Mutant *Bacillus paralicheniformis* MT039446.1

Sikander Ali,[a,*] Muhammad Usman Ahmad,[a] Maryam Naz,[a] Farheen Afzal,[a] Majid Khan,[b] Nawal H. Sidig,[c] Nawal Al-Hoshani,[d] Nouf Ali Asiri,[e] Aala A. Abulfaraj,[f] and Tariq Aziz [g,*]

Acetoin is a valuable by-product of glucose metabolism with wide applications in the chemical, food, cosmetic, and pharmaceutical industries. This study investigated acetoin production using both wild-type and mutant strains of *Bacillus paralicheniformis* MT039446.1. Production was optimized by varying incubation time to determine conditions that maximized yield. UV-visible spectroscopic analysis showed distinct absororption peaks at 350 nm for the wild strain and 450 nm for the resistant mutant strain. Functional group characterization was further validated using Fourier transform infrared analysis confirmed the presence of carbonyl compounds. Structural and morphological changes in the solid substrate (press mud) during fermentation were examined through scanning electron microscopy and X-ray diffraction techniques, indicating substrate modification during microbial activity. Kinetic analysis demonstrated a significant improvement in the mutant strain (NA-cys3), with volumetric productivity (Qp) reaching 0.33 g/L·h compared to 0.16 g/L·h in the wild strain. This enhancement reflects improved efficiency of the acetoin biosynthetic pathway following mutagenesis. Overall, the study highlights an environmentally sustainable and economically viable approach for acetoin production using agro-industrial waste. This strategy supports the development of circular bio-economy models and offers potential for scalable bio-manufacturing applications.

DOI: 10.15376/biores.21.4.9962-9984

Keywords: Acetoin; Bacillus; Fermentation; Kinetics; Statistical analysis

Contact information: a: Department of Microbiology, Ikram-Ul-Haq Institute of Ind. Biotechnology (IIB), GC University Lahore, Pakistan; b: Institute of Biotechnology and Genetic Engineering, The University of Agriculture, Peshawar, 25120, Khyber Pakhtunkhwa, Pakistan; c: Department of Mathematical Sciences, College of Science, Princess Nourah bint Abdulrahman University, P.O. Box 84428, Riyadh 11671, Saudi Arabia; d: Department of Biology, College of Science, Princess Nourah bint Abdulrahman University, P.O. Box 84428, Riyadh 11671, Saudi Arabia; e: Department of Environmental Sciences, College of Science, University of Jeddah, Jeddah, Saudi Arabia; f: Biological Sciences Department, College of Science & Arts, King Abdulaziz University, Rabigh 21911, Saudi Arabia; g: Biodiversity Genomics Unit, University of Tabuk, 71491, Tabuk, Saudi Arabia;

** Corresponding authors: dr.sikanderali@gcu.edu.pk; tariqckd@ut.edu.sa*

INTRODUCTION

Acetoin finds its applications best in the chemical, food, cosmetics, and pharmaceutical industries (Zhu *et al.* 2016). In the chemical industry, acetoin is used as a precursor for the production of diacetyl (2,3-butanedione) (Yang *et al.* 2017). Diacetyl is an important flavoring compound widely used to impart buttery and creamy notes to food

products, including butter, margarine, dairy products, bakery products, confectionery, popcorn, and snack foods. It is also used in flavor and fragrance formulations because of its characteristic buttery aroma (Xiao and Lu 2014a). These traits also help in its use in a variety of fermentative foods and beverages (Xiao and Lu 2014b). Acetoin is a naturally occurring compound that is widely present in various foods and biological materials. Synthetic acetoin is also used as a flavoring and fragrance ingredient in the food and cosmetic industries. In contrast, bio-based production of acetoin from renewable substrates provides a sustainable route for its production and offers potential for its use as a platform chemical for the synthesis of value-added compounds, such as 2,3-butanediol. (Li *et al.* 2014). Because of all these high-value usages of acetoin in various industries, it is characterized as a top 30 platform chemical by the United States Department of Energy (DOE) (Xiao and Lu 2014a). Current production of acetoin mostly involves the use of fossil fuels and oils. However, climate changes led by global warming and greenhouse gas effects have encouraged the need to switch from chemical to microbial processes of acetoin production, ensuring sustainable development processes (Lee *et al.* 2021). Acetoin is a microbial fermentation product synthesized by several bacterial species through the metabolic conversion of carbohydrates into pyruvate-derived intermediates (Sharma *et al.* 2020).

Fermentation can be classified into three main types based on the physical state of the substrate: solid-state fermentation (SSF), submerged fermentation (SmF), and semi-solid fermentation. In solid-state fermentation (SSF), microorganisms grow on a moist solid substrate that contains little or no free water. The solid material serves both as a physical support and as a source of nutrients for microbial growth, while the limited moisture content distinguishes SSF from other fermentation methods (Yafetto 2022). In contrast, submerged fermentation (SmF) is carried out in a liquid nutrient medium in which microorganisms are completely immersed. The liquid medium provides all the essential nutrients required for microbial growth and metabolism, enabling efficient production of a wide range of metabolites. Owing to its ease of process control and scalability, SmF is widely employed for the industrial production of secondary metabolites, including antibiotics, as well as primary metabolites such as alcohols and organic acids (Gong *et al.* 2023). Lastly, semi-solid fermentation is defined as an intermediate of the above two types as it requires more moisture content than SSF but is less submerged than SmF. It is often used for starter culture productions or some probiotics (Śliżewska and Chlebicz-Wójcik 2020). All three fermentation processes hold great value.

Glucose is often regarded as an easy option as a substrate, although it is relatively expensive to be used in industry. However, certain biofuels are found to be more useful in this aspect. This includes lignocellulosic materials, molasses, seaweed hydrolysate, and soybean meal hydrolysate. All are more economical than glucose (Yang *et al.* 2016). Plants biomass, such as crops, agricultural residues, wood, algae, *etc.*, are used in acetoin production using SSF (Jia *et al.* 2017).

In present study, press mud was used as the substrate. The press mud (also known as filter cake or filter press cake) is a solid by-product generated during the clarification of sugarcane juice in sugar mills (Solomon 2016). It is produced after the addition of lime and other clarifying agents, followed by filtration of the precipitated impurities. Typically, press mud constitutes approximately 3 to 5% of the total weight of crushed sugarcane and contains abundant organic matter, residual sugars, cellulose, hemicellulose, lignin, proteins, waxes, and essential macro- and micronutrients, including nitrogen, phosphorus, potassium, calcium, magnesium, iron, and zinc (Dotaniya *et al*. 2016; Solomon 2016).

Owing to its rich nutrient composition, low cost, and widespread availability, press mud has emerged as a promising agro-industrial substrate for microbial fermentation and the production of value-added bioproducts. Its utilization not only enhances the economic feasibility of fermentation processes but also promotes sustainable waste management through the valorization of sugar industry residues (Pandey *et al.* 2000; Chandel *et al.* 2018). Among various agro-industrial residues, press mud generated by the sugar industry represents an abundant and nutrient-rich biomass with considerable potential for microbial bioprocesses. Valorization of press mud through microbial fermentation enables the production of value-added chemicals while simultaneously addressing environmental concerns associated with its disposal (Solomon 2016; Dotaniya *et al.* 2016).

The analytical evaluation of the samples is done by characterization processes. Ultraviolet-Visible (UV-Vis) spectroscopy is a simple, quick, and cheap technique that does not need much calibration to characterize certain samples (Singh *et al.* 2024). Unfortunately, there is an overlapping of absorbance bands in the UV-Vis range making it difficult to analyze samples (Vogt *et al.* 2023). Fourier transform infrared spectroscopy (FTIR) is also used to determine any changes in biomolecules by analyzing changes in functional groups (Eid 2022). However, it is unable to assess the purity of a substance if certain parameters are unknown (Mourdikoudis *et al.* 2018). Another technique, X-ray diffraction analysis uses the pattern of ray refractions for these determinations (Fatimah *et al.* 2022). XRD works on Bragg's law (Thakar *et al.* 2022). Scanning electron microscopy (SEM) is used to obtain surface and elemental images of substances in high resolution. SEM is a surface imaging method with high resolution microscopy. This technique analyzes shapes, size distribution, and topography (Ural 2021). It is also seen to resolve different particle sizes (Chandra *et al.* 2014). SEM can degrade components of the samples but careful handling can overcome this drawback (Relucenti *et al.* 2021).

Kinetic studies are essential to find rates of reaction and the variables that effect these rates. There are various models of kinetic studies and parameters. Key parameters include specific growth rate (SGR), product and growth yield coefficients, volumetric rates and specific rate constants. The SGR is an important kinetic parameter that is often expressed in relation to doubling time as a ratio of biomass formation to doubling time of biomass (Nielsen 1999). Yield coefficients from yield equation play a vital role in determining reducing power balances, ATP production, and overall metabolic efficiency of cells (Andrews 1993). Volumetric rates including product formation (Q_p), biomass formation (Q_x), and substrate consumption (Q_s) are also crucial for metabolic determination of product, biomass, and substrate, respectively. In parallel, specific rate constants are determined for product formation (q_p) and substrate consumption (q_s). These constants represent the processes on a per-unit biomass basis, typically expressed per hour. Collectively, these parameters enable a comprehensive mathematical description of biomass production, substrate consumption, and product synthesis over time forming the basis of kinetic studies (Xu *et al.* 2021).

Acetoin production in this research protocol involved novel approaches. Press mud was used as substrate for fermentation. *Bacillus paralicheniformis* was used to produce acetoin in this protocol. Although *B. paralicheniformis* has the metabolic pathway for acetoin biosynthesis as part of 2,3-butanediol fermentation, it has not been widely reported as a major acetoin-accumulating strain under standard conditions. The mutagenesis of the bacterial strain using nitrous acid and further inducing resistance in the mutant strain for improving yield makes this protocol more original and unique.

EXPERIMENTAL

Chemicals and Glassware

The chemicals used in this research work were obtained from companies including Acros Organics, Daejung Chemicals, Sigma-Aldrich, and Fisher Scientific. All the chemicals and glassware were collected from the Department of Microbiology, Dr. Ikram-Ul-Haq Institute of Industrial Biotechnology (IIB), GC University, Lahore. The chemicals that were used in this research work were of analytical grade.

Microorganism and Culture Maintenance

The culture of *Bacillus paralicheniformis* MT039446.1 was obtained from Microbial Culture Bank, IIB, GCU, Lahore. The Luria-Bertani (LB) agar medium was used for bacterial culturing and the slant cultures were incubated under optimum conditions at 37 ℃ for 16 to 20 h. The pre-grown slants were stored at 4 ℃ for future use, ensuring the viability of the bacterial strain.

Fermentation Procedure

Fermentation inoculum was prepared in two steps involving pre-seed and post-seed cultures in LB broth and glucose mineral salts (GMS) medium, respectively, with incubation under shaking conditions. Optical density was standardized ($OD_{600} \approx 1$) to maintain consistent cell concentration. Solid-state fermentation (SSF) was then carried out using press mud as substrate, moistened with GMS medium, sterilized, inoculated, and incubated at 37 °C. Post-fermentation, acetoin was extracted into the aqueous phase, centrifuged, and stored for analysis. Quantification of acetoin was performed using the modified Voges–Proskauer method, while residual glucose was estimated using the DNS method (Jia *et al.* 2017).

To enhance acetoin production, process optimization was conducted by varying substrate concentration, moisture ratio, glucose levels, inoculum size, and incubation time. Additionally, strain improvement was achieved through HNO_2-induced mutagenesis followed by screening for improved yield mutants and development of L-cysteine HCl resistance. The most efficient mutant strain (NA-cys3) was selected and further optimized alongside the wild-type strain under SSF conditions (Xu *et al.* 2022).

Acetoin Extraction Method

The acetoin was extracted by the method explained by Jia *et al.* (2017) and Xu *et al.* (2022).

Optimization of Resistant Mutant Strains

The resistant mutant stain (NA-cys3) along with wild-type strain (MT039446.1) was made to increase acetoin production by optimization of time of incubation. The different times of incubation (12, 24, 36, 48, 60, and 72 h) of inoculated fermentation mixture were investigated for MT039446.1 and NA-cys3 strain of *B. paralicheniformis* under already optimized conditions of SSF (Singh *et al.* 2018). The growth $OD_{575\ nm}$ was measured and results were noted carefully for further use in kinetic studies.

Characterization of Substrate and Product

The samples were analyzed for their morphological, structural, functional, and optical properties using modern techniques. The samples were evaluated using UV-Vis

spectroscopy (Mao *et al.* 2017). The UV-Vis spectrophotometer (Cary 60, Version 2 UV–Vis Spectrophotometer; Agilent Technologies, Santa Clara, CA, USA) was carried out in the Nanotechnology Laboratory of Chemistry Department at GC University, Lahore. A quartz cuvette with a path length of 1 cm carrying 3 mL of each prepared sample was used. Distilled water was used as a blank. The absorption spectra were secured in a digital device and observed.

The samples were sent to the Department of Chemistry, UET Lahore for FTIR analysis. The FTIR Cary 630 (Agilent Technologies, Santa Clara, CA, USA) was used. The samples were placed on the sample holder. FTIR analysis was performed using the attenuated total reflectance (ATR) method. The samples were directly placed on the ATR crystal, and the spectra were recorded over the range of 4000 to 400 cm^{-1} with a spectral resolution of 4 cm^{-1} and 32 scans per sample .The temperature was set at 25 °C (Kartika *et al*. 2026). The infrared beams were passed from the samples, which resulted in the formation of spectra that was recorded by the detector and was plotted on Origin software (Cole *et al.* 2017).

Post-fermentation press mud sample was sent to Department of Chemistry, University of Engineering and technology, Lahore for structural examination by X-ray diffraction. The analysis was done using Cu Kα radiation (λ = 1.5406 Å) operated at 40 kV and 30 mA (Gupta *et al.* 2011). Finely ground samples were prepared for analysis and underwent XRD conducted over a 2θ range of 20° to 80° with a step size of 0.02° and a scanning rate of 2° min^{-1}. Observations of spectra were recorded, and graphs were prepared using Origin software (Sivagurunathan *et al*. 2026).

The size, surface arrangement and shape of both samples were observed under SEM (Gumanta *et al.* 2023). Samples were sent to CASP, GC University, Lahore for SEM (EVOLS10, ZEISS Company Carl Zeiss AG, Oberkochen, Germany) operated at 10 kV with a secondary electron detector.

Samples were mounted on aluminium stubs using conductive carbon tape and sputter-coated with a thin layer of gold prior to imaging. The sample was placed on the chamber, stage was maintained, and different angles were collected. An intense beam of electrons scanned the samples. It produced many signals that were picked up by the SEM device. It produced a replica of the sample surface. The resulting images were then observed and compared (Afzal *et al.* 2026).

Kinetic Parameters

The kinetic parameters were analysed for the fermentation of acetoin production by wild-type (MT039446.1) and putative mutant strain (NA-cys3) *B. paralicheniformis* using press mud as a carbon source under SSF. The procedures of Pirt (1975) and Lawford and Roseau (1993) were adopted. Product formation (Q_p) and substrate consumption (Q_s) volumetric rates were calculated from the plots highest slopes of acetoin produced and substrate utilized each *vs.* the fermentation time. Biomass formation (Q_x) volumetric rate was determined from the plotted highest slope of the formation of cell mass and time period of incubation. Product formation (q_p) and substrate consumption (q_s) specific rate constants were calculated from respective equations, *i.e.*, $q_p = \mu \times Y_{p/x}$, $\mu \times Y_{p/s}$, and $q_s = \mu \times Y_{s/x}$. The formation of cell mass (q_x) specific rate constants was determined by the yield coefficient of growth ($Y_{x/s}$) multiplication with the specific growth rate (μ).

The one-way analysis of variance (ANOVA) (version-4, SPSS-9) followed by *post hoc* multiple comparisons was performed to understand the change in acetoin

production by MT039446.1 and NA-cys3 strain of *B. paralicheniformis* under SS (Snedecor and Cochran 1980). The experiments were performed in triplicate and results were expressed as mean ± standard deviation (SD).

RESULTS AND DISCUSSION

Optimization of Fermentation Conditions for the Mutant Bacterial Strain

Effect of time of incubation

The time of incubation was found to affect biomass formation, sugar consumption, and acetoin production, as investigated from 12 to 72 h (Fig. 1). There was an increase in biomass formation of NA-cys3 from 0.86 to 2.22 between 12 and 48 h. After 48 h, the OD started decreasing. It was also observed to be nearly constant from 36 to 72 h. The biomass formation of wild-type *B. paralicheniformis* also rapidly increased from 12 to 48 h.

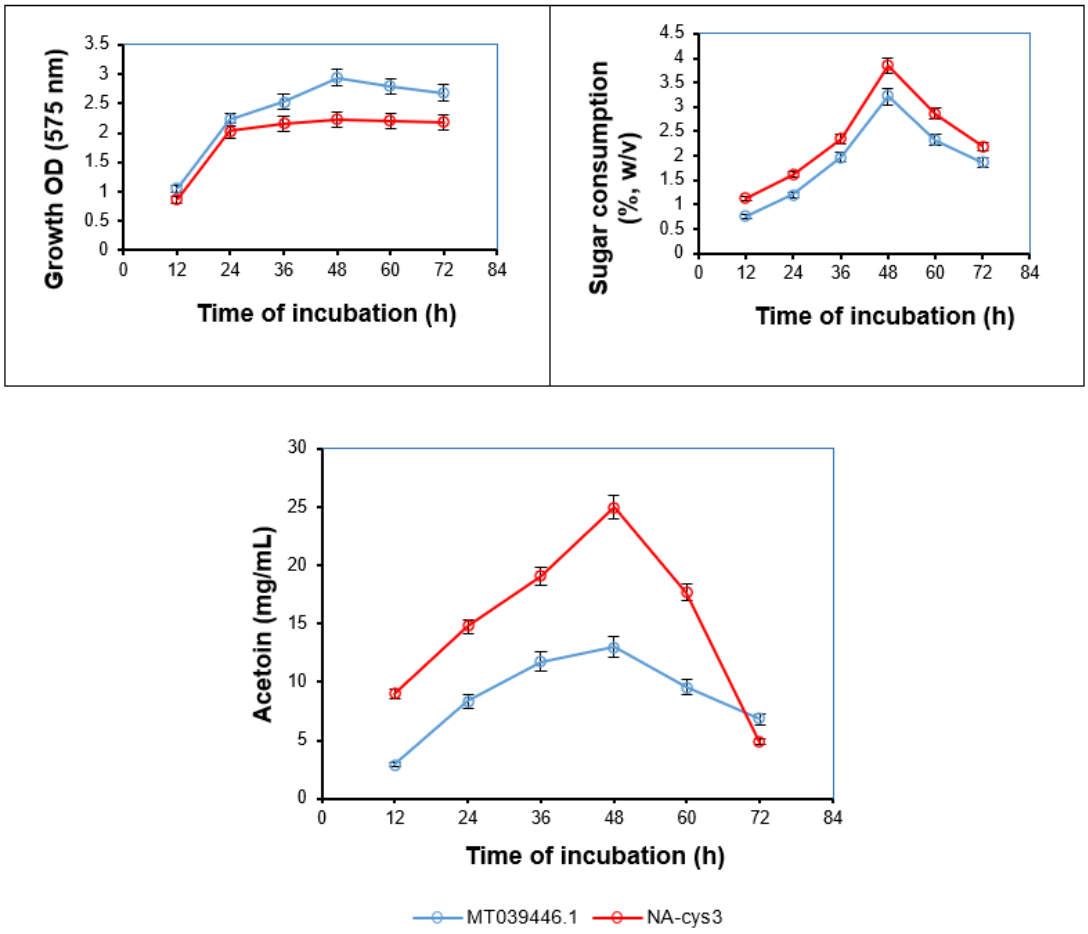

Fig. 1. Effect of different time of incubation on biomass formation, sugar consumption, and acetoin production by wild-type (MT039446.1) and putative mutant strain (NA-cys3) *B. paralicheniformis* under SSF

The highest growth OD (2.94) was demonstrated at 48 h time of incubation. Similarly, the graph showing sugar consumption over various time of incubation (12, 24, 36, 48, 60, and 72 h) demonstrated the same trend of steady increase in sugar consumtion until 48 h for both wild-type (0.76 to 3.21%, w/v) and putative mutant strain (1.12 to 3.85%,

w/v). After that, sugar consumption started decreasing with time. Lastly, effect of different times of incubation on acetoin production was studied. The graph showed an increase in acetoin (8.98 to 24.97 mg/mL) until 48 h for the NA-cys3. After this time of incubation, the production decreased. The wild-type *B. paralicheniformis* demonstrated the same trend but the slope was steady compared to putative mutant strain. Therefore, optimum time of incubation was chosen to be 48 h.

This trend was consistent with reports of *Bacillus* behavior: acetoin (and 2,3-butanediol) are often produced during mid growth then repressed as the culture enters the stationary phase or shifts carbon flux toward other pathways. As an illustration, a wild strain of *B. subtilis* yielded the maximum amount of acetoin after 24 h (Bibra *et al.* 2018), whereas the rest had their peak after 60 to 72 h (Jia *et al.* 2017). This study showed optimal results (48 h) falling between these two extremes. This indicated that in these strains both the speed of acetoin production and its metabolic control present a trade-off between their rapid production and conversion to be used or directed towards another chemical. These findings validate that the best acetoin produced by both the strains was at 48 h of fermentation. This was also in line with the report of Tian *et al.* (2016), who cited high capacities of bioacetoin production by *Bacillus* after 72 h, which could, however, be linked to the strain-specific kinetics or medium itself. Further, the genetically modified strain of *Saccharomyces cerevisiae* provided an elevated production of bioacetoin in 55 h production period than the batch flask fermentation of 48 h (Bae *et al.* 2016), which shows that extensive production periods can be calibrated by feeding patterns. Similarly, Ji *et al*. (2011) reported that strain improvement and optimization of fermentation parameters significantly enhanced acetoin productivity in *Bacillus* spp., highlighting the importance of microbial strain selection for industrial bioprocesses.

Table 1. Common Experimental Conditions Used for All Experiments

Parameters	Conditions
Temperature	37 °C
Press mud	40 g
Substrate to diluent ratio	1:1`
Inoculum size	5%
Glucose concentration	5%
Replicates	3 independent replicates
Statistical analysis	One way ANOVA
Significance Level	$p \leq 0.05$
Error bars	Standard deviation

Characterization of Press Mud and Acetoin

Ultraviolet-visible (UV-Vis) spectroscopy of acetoin

Figure 2 compares absorbance spectra of acetoin samples of both the wild-type and mutant strains. The spectra in each of the cases show intense absorbance at 375 and 475 nm, respectively. This indicated the presence of the alpha-hydroxy ketone functional group, present in acetoin. There was also a significant difference in the absorbance of wild-type and mutant and this difference suggested that the acetoin concentration increases after mutation. The general spectral profiles of both wild-type and mutant samples were quantitatively equivalent, except that the intensity is where substantial disparity was noted; the optimized spectrum of the mutant had the highest peak, second only to the optimized

wild-type overall. The similarity of the spectral characteristics of wild-type and mutant sample indicates that the mutant did not cause the appearance of additional byproducts, which are detectable by UV-Vis; instead, both wild-type and mutant strains synthesized the same acetoin in terms of its chemistry. This would mean that this optimization touched on quantity thereby not purity (Picollo *et al.* 2019). The lack of extra peaks was evidence that there is little contamination by strongly absorbing impurities. Therefore, the UV-Vis is reliable to show the presence of acetoin. The outcomes justify the conclusion of increased acetoin yield during optimization with no changes in the chemical structure.

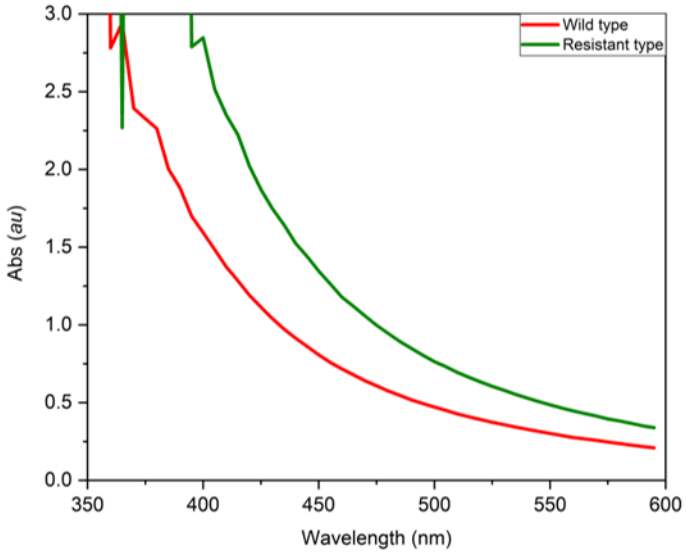

Fig. 2. Comparison of UV-Vis spectroscopy of pre-optimization acetoin and post-optimization acetoin produced by wild-type (MT039446.1) and putative mutant strain (NA-cys3) *B. paralicheniformis* under SSF

FTIR Analysis of Acetoin

Figure 3 displays FTIR spectra of wild type and resistant strain samples of acetoin production. Similar characteristic absorbance bands were observed in all spectra, which attested to the identical structure of the molecule. The band at 3300 to 3400 cm^{-1} present in all samples indicated O-H vibration of the 3-hydroxy group in acetoin. Each spectrum shows a sharp peak, which is the ketone stretch of C=O observed around 1720 cm^{-1}. The peak at around 2960 to 2870 cm^{-1} is due to methyl C-H stretching vibrations of methyl groups. It also contains bending vibrations of $-CH_3$ at 1380 to 1450 cm^{-1} and C-O or C-C stretch at 1050 to 1150 cm^{-1}. No new bands were found in the samples, but differences occurred mainly at relative intensities. Generally, the spectra after optimized condition recorded minor intensities of -CH and C=O bands, which is in line with increased concentration of acetoin. The location of the peaks in the wild-type samples and the mutant samples were almost same, and this relationship implied that the samples shared the identical functional groups. Small differences (*e.g.*, small changes in the O-H bandwidth) would probably indicate changes in concentration or hydrogen bonding. The FTIR spectra identified the functional groups of acetoin (Nandiyanto *et al.* 2019). The respective O-H stretching and C = O stretching bands observed were the expected ones against 3-hydroxy-2-butanone.

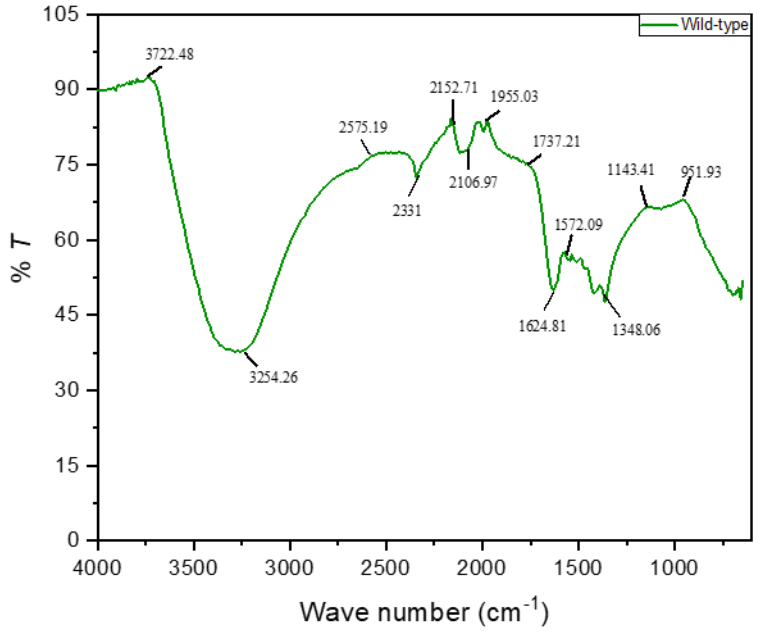

Fig. 3. FTIR analysis of post-optimization acetoin produced by wild-type (MT039446.1) *B. paralicheniformis* under SSF

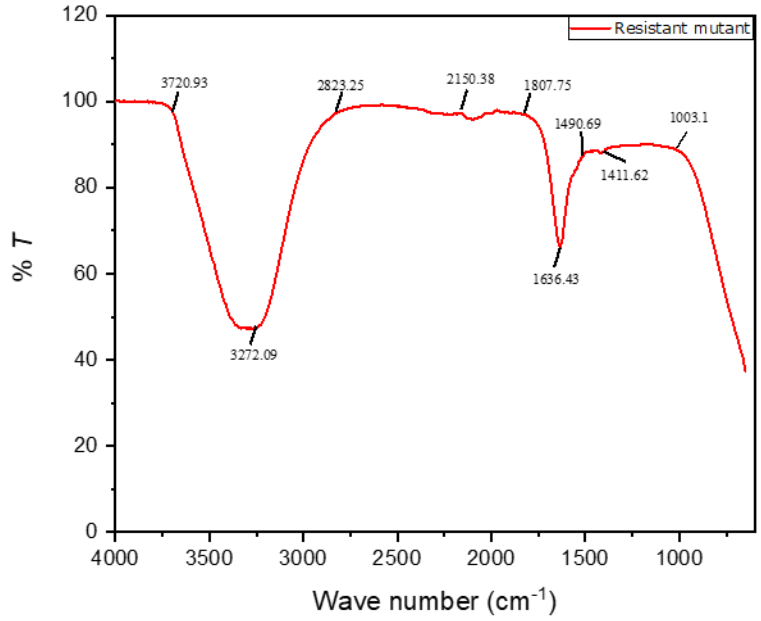

Fig. 4. FTIR analysis of post-optimization acetoin produced by resistant mutant strain (NA-cys3) *B. paralicheniformis* under SSF

Afshar *et al.* (2014) reported that press mud has free and hydrogen-bonded OH groups that would be located within the same area. Likewise, there is a hydroxyl group of acetoin expressed at about 3300 cm^{-1}. The ketone carbonyl stretch near 1720 cm^{-1} is also a characteristic functional group of acetoin. Saini *et al.* (2023) suggested that FTIR be used to determine the structural changes, such as pretreatment of lignocellulosic biomass that typically removes lignin peaks in the fingerprint region. Here, the press mud had its own FTIR peaks but the analyzed samples contain the acetoin product of both wild and resistant

bacteria (Cole *et al.* 2017). The consistency of peak positions across all samples confirms that both wild-type and mutant strains produced identical acetoin molecules. Overall, the FTIR data support the conclusion that mutation improved acetoin production and did not introduce new chemical species. It indicated the presence of acetoin that had been produced by both wild and mutant strains.

X-Ray Diffraction Analysis of Press mud

In Fig. 5, XRD patterns of the sugarcane press mud substrate post-fermentation SSF with the mutant strain are shown. Specifically, the peaks at 22 to 29° showed the presence of calcite ($CaCO_3$) and at 26 to 27° illustrated the presence of quartz (SiO_2). These characteristics showed that the press mud was composed of calcium carbonate and silica-rich residue. No additional peaks and other crystalline phases were identified. This indicated an incomplete loss of amount of crystalline organic. The fact that the main mineral peaks were still apparent signifies that the SSF process had not led to perturbations across the inorganic matrix of the press mud, yet selective break down of fermentable organic materials only took place. Results of XRD analysis show that, by and large, crystalline minerals in pressed mud remain after fermentation. This observation is parrallel to the observation by Afshar *et al.* (2014). This suggested that sugarcane press mud contains plenty of calcite, hematite, and quartz. Fermentation probably proceeded in the amorphous or poorly crystalline organics (*e.g.*, cellulose, hemicellulose), and this would give rise to diffuse or low-intensity diffraction that may be gone. It was parrallel to the finding of Khan *et al.* (2020) that the minor decrease in some maximum values was due to microbial decomposition of biomass. The absence of novel diffraction peaks demonstrated the absence of novel inorganics, such as byproducts of fermentation, that lead to the crystallization entered production during SSF (Jha *et al.* 2019).

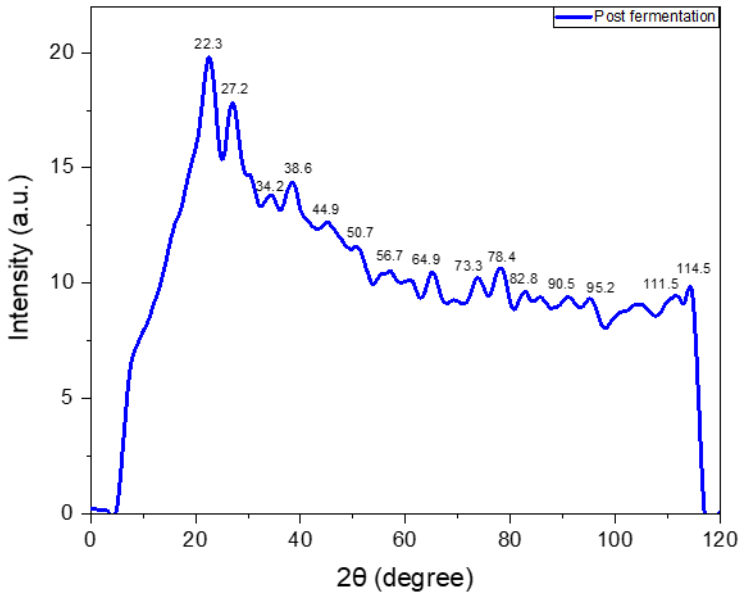

Fig. 5. X-ray diffraction analysis of substrate for post-fermentation press mud produced by putative mutant strain (NA-cys3) *B. paralicheniformis* under SSF

SEM Analysis of Press Mud

As illustrated in Fig. 6, SEM micrographs of press mud substrate before the fermentation were obtained (wild type inoculum). The photographs show that the raw press

mud particles had a discontinuity that was relatively smooth. The aggregates are dense and not a regular shape, and there was no sign of bacterial colonisation. Its morphology resembled that of sun-dried control press mud. SEM analysis in previous studies has shown that the untreated substrate exhibits a relatively smooth and intact surface morphology (Nimbalkar *et al.* 2017). Fine particulate matter and textural plant fiber remained but not deep fissures or enormous pores in the total surface. In the high-magnification SEMs, a bit of texture was apparent at a micron scale, although the material was mostly consolidated. This was considered as a baseline SEM morphology that was used as a reference source to changes that occur after SSF (Welden *et al.* 2022). The outcome of the SEM images of the untreated press mud taken before fermentation verifies there was no change in the surface structure of the mud. There was no visible biotic characteristics, for *a priori* fermentation was at an early stage. On similar note, Nimbalkar *et al.* (2017) noted that the control press mud in sun-dried morphology was smooth and intact. The microbial action therefore altered the SEM, which acted as a baseline.

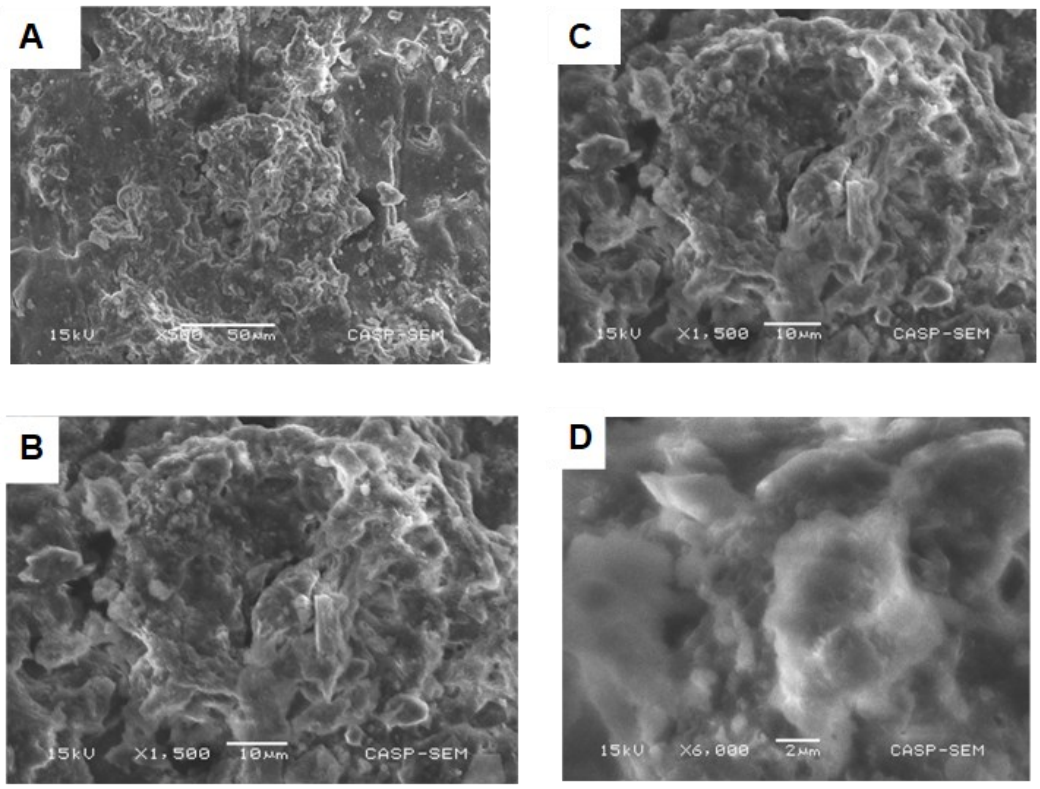

Fig. 6. Comparison of SEM scans of press mud pre fermentation and post-fermentation, (A) pre fermentation press mud at 500X magnification (B) pre fermentation press mud at 1500X magnification (C) post fermentation press mud at 1500X (D) post fermentation press mud at 6000X

The whole inorganic and fibrous matrix implies that the substrate did provide uninterrupted surface that microbes could attach to initially. The functional groups introduced by press mud, *e.g.*, hydroxyls, carbonates, are presumably reactive in relation to early moisture retention. However, they did not command influential changes in solid-phase morphology. This baseline is of significance in fermentation studies as reported by Ural (2021) because, once maintained, a disrupted surface occurs. Hence, in this case, the SEM findings align with a situation where crude biomass was physically homogenous up

to the time when microorganisms started its degradability. Such findings were consistent with those of other studies of biomass, as in the study of Harish *et al.* (2017), in which raw lignocellulosic wastes demonstrated compact-particles before developing into porous ones due to microbial treatment. Overall, the SEM revealed that the press mud did not have a structurally degraded form in the time span before fermentation.

Kinetic Parameters

Time course comparison for volumetric rates

Figure 7 compares the volumetric rates, *i.e.*, Q_x (biomass formation, in OD/h), Q_s (substrate consumption, % w/v per h), and Q_p (product formation, mg/mL/h) for the both wild-type and resistant mutant strains. Q_x was observed to increase from 0.022 to 0.061 OD/h between 12 to 48 h for wild-type.

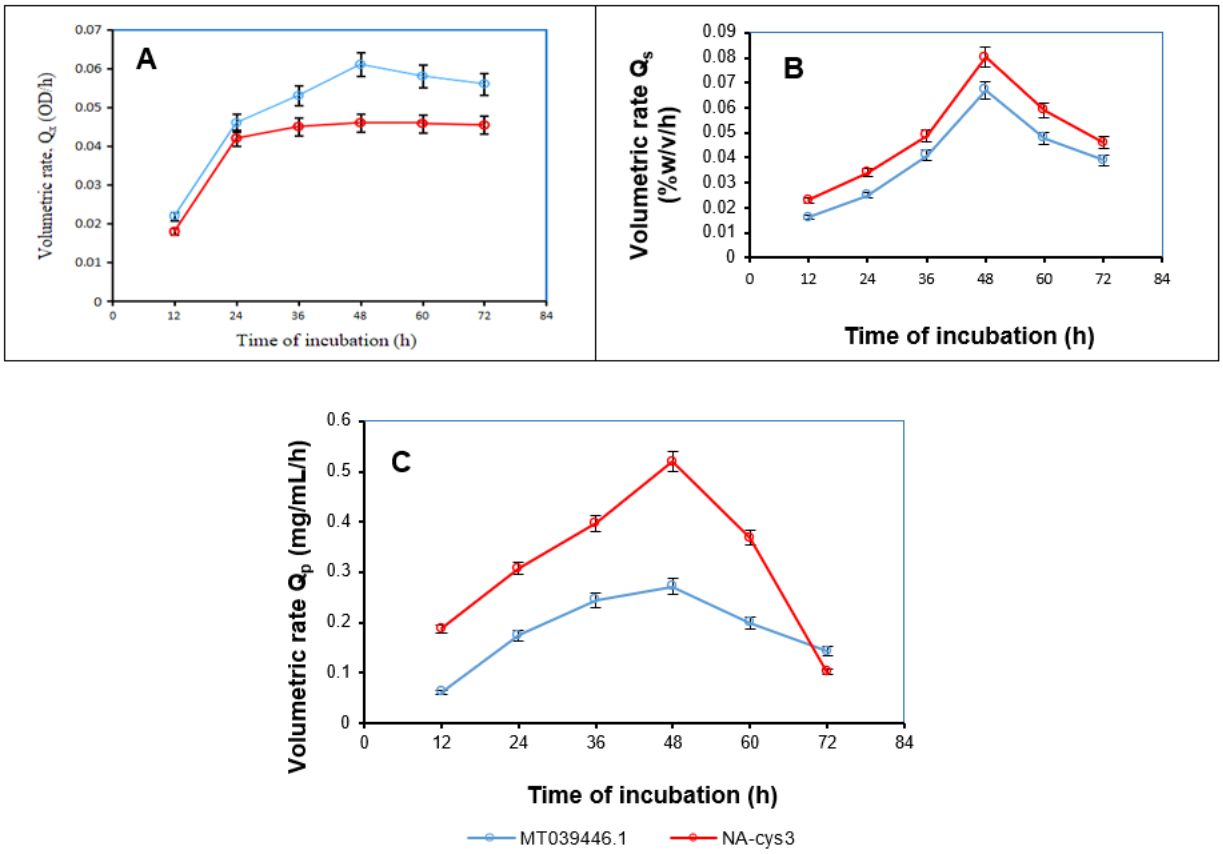

Fig. 7. Comparison of volumetric rates over different time courses for acetoin production by wild-type (MT039446.1) and putative mutant strain (NA-cys3) *B. paralicheniformis* under SSF

After 48 h, a slight decrease in Q_x was observed. Resistant mutant strain followed the same trend but a minor decrease in Q_x after 48 h was observed. Q_s similarly peaked at 48 h (wild type 0.067 ± 0.02%/h; mutant 0.0802 ± 0.03%/h) and then dropped sharply as time of incubation was increased till 72 h. Unlike Q_x, Q_s showed higher values for NA-cys3 than wild-type. Simultaneouly, Q_p (mg/mL/h) also demonstrated peak value at 48 h, *i.e.*, the wild-type Q_p was 0.271 ± 0.005 mg/mL/h, whereas the mutant Q_p was 0.52 ± 0.004 mg/mL/h ($p \leq 0.05$). Q_p decreased after 48 h and reached the lowest (0.102 mg/mL/h for NA-cys3) at 72 h. Q_p also demonstrated higher values for resistant mutant strain. These patterns indicated that the wild-type strain converted biomass and substrate into acetoin

more rapidly. The volumetric rates (biomass formations (Q_x), substrate consumption (Q_s), and product formations (Q_p)) were compared to give a concise picture of metabolic efficiency and metabolic productivity of wild type and mutant *B. paralicheniformis* (NA-cys3).

Lee *et al.* (1999) reported the sub-optimal metabolic conversion hypothesis by the mutant was also supported by raised Q_s levels without relevant increase in biomass production. The largest difference between the strains was in product formation rate (Q_p), in which the mutant showed a much higher rate at its peak (48 h) although this had a lower biomass. Bentley *et al.* (1990) indicated that the mutation could increase in the passage through the biosynthetic route towards the production of the target product perhaps by derepression or changing regulation. The decrease of Q_p beyond 48 h in the two strains however indicated the presence of feedback inhibition or product toxicity. Overall, these findings indicate that these NA-cys3 mutants grew less efficiently, yet they could have a productivity potential as far as the optimized conditions were met.

Time Course Comparison of Specific Rate Constant (q_p)

Comparison of specific rate constants for product formation q_p (µg/L/h) for $\mu \times Y_{p/x}$ and $\mu \times Y_{p/s}$ respectively, over different time courses for acetoin production by wild-type (MT039446.1) and putative mutant strain (NA-cys3) *B. paralicheniformis* under SSF, as shown in Fig. 4.7a. First, the q_p increased from 0.551 to 0.615 µg/L/h between 12 h and 24 h NA-cys3. The q_p then decreased between 24 and 36 h, remaining almost constant from 36 to 48 h. After 48 h, a sudden decrease in q_p was observed from 0.517 µg/L/h at 48 h to 0.069 µg/L/h at 72 h. The wild-type (MT039446.1) also increased between 12 to 24 h. The q_p kept decreasing after that to 0.094 µg/L/h at 72 h. The specific rate constant for product formation q_p ($\mu \times Y_{p/s}$) showed an increasing trend from 12 to 24 h for both strains. After that, it kept decreasing till 72 h (0.135 µg/L/h for MT039446.1 and 0.069 µg/L/h for NA-cys3). The time course of the particular product formation rate q_p of the wild-type and NA-cys3 strains fit into a classical microbial fermentation kinetic regime in which q_p increased during the active growth phase, and then decreased due to cells moving into stationary state and substrate limitation. This variation can be due to changes in cofactor availability or changes in allocations of the down stream pathways caused by mutation-driven shifts in redox balance or regulation of enzymes.

Similar trends had been reported in *Bacillus* fermentations by Wang *et al.* (2025). The volumetric productivity of the wild-type *B. subtilis* peaks and then declined precipitously in batch cultivations. However, the productivity of engineered strains in which genes of acetoin pathway were over-expressed remained high later. Metabolic reconfiguration had also produced high volumetric productivities (> 2 g/L/h) in *B. licheniformis* fed-batch cultures, and this modulation of the genetic enhancement was reflected by Gui *et al.* (2020) as how q_p kinetics occur both in shape and persistence. These experiments served to emphasize that the resulting outcome of kinetic path observed corresponds both to homeostatic physiological constraints as well as strain-specific optimizations of metabolic consumptions. Finally, although both strains exhibit fermentation kinetics, it could not be ignored that the mutant possessing lower q_p indicated an additional requirement to accommodate a higher flux control and redox balance used to maintain its productivity.

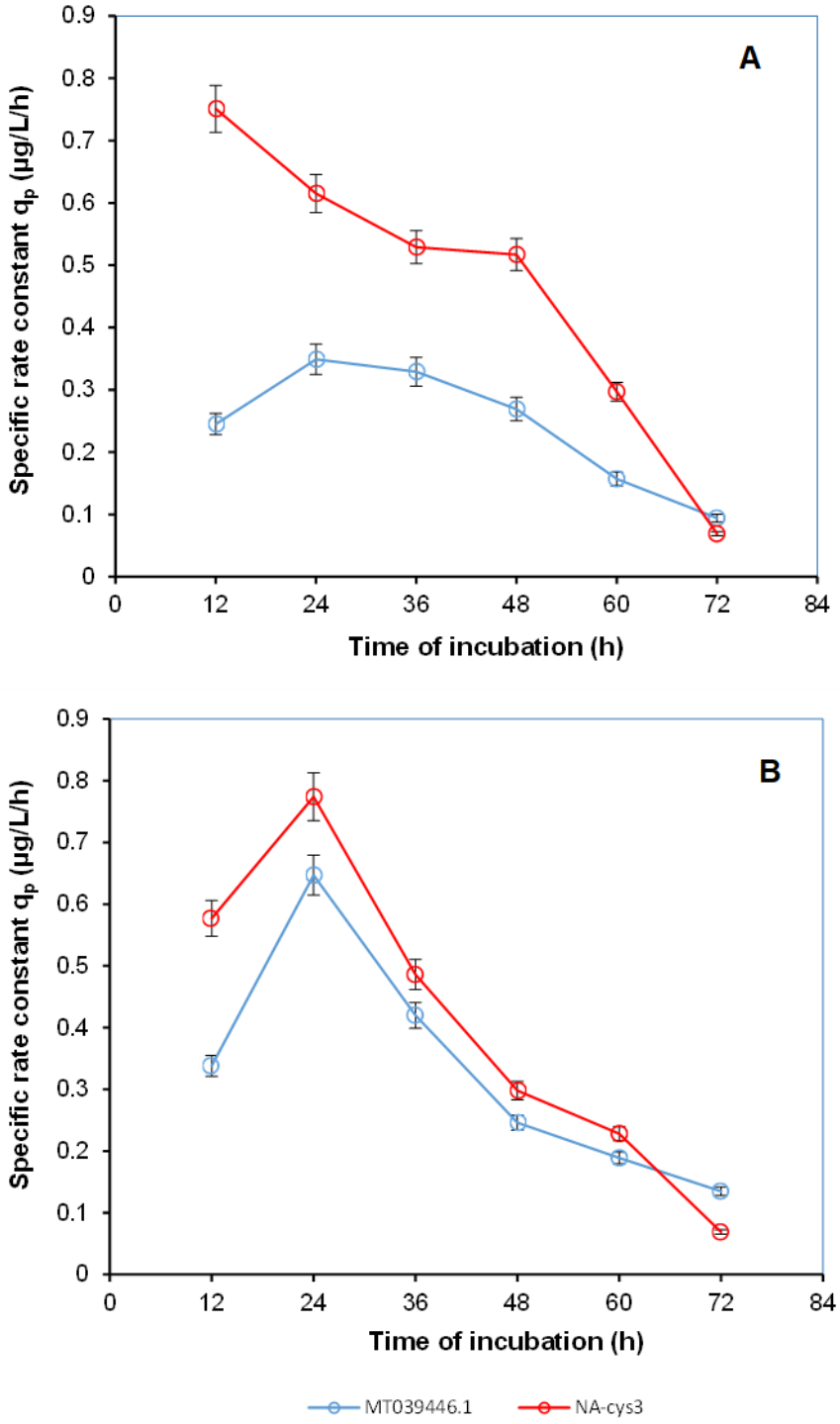

Fig. 8. Comparison of specific rate constants over different time courses for acetoin production by wild-type (MT039446.1) and putative mutant strain (NA-cys3) *B. paralicheniformis* under SSF; Temperature 37 °C, press mud as substrate 40 g, substrate to diluent ratio 1:1, inoculum size 5% (v/w), glucose conc. 5% (w/v); Kinetic parameters: Specific rate constant for product formation = q_p (µg/L/h) for $\mu \times Y_{p/x}$ and $\mu \times Y_{p/s}$, respectively

Time Course Comparison of Specific Rate Constant (q_s and q_x)

Figure 9 compares the specific rate constants for biomass formation q_x (µg/L/h) and specific rate constants for substrate consumption q_s (µg/L/h), over different time courses

for acetoin production by wild-type (MT039446.1) and putative mutant strain (NA-cys3) *B. paralicheniformis* under SSF. First, the q_x increased from 0.121 to 0.172 µg/L/h between 12 h and 24 h, MT039446.1.

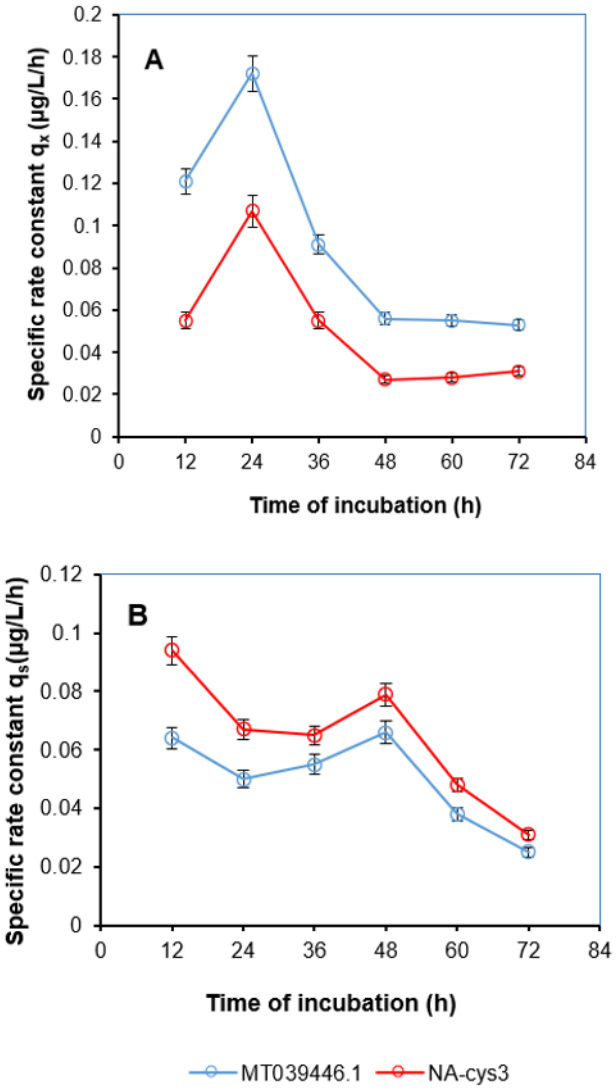

Fig. 9. Comparison of specific rate constants over different time courses for acetoin production by wild-type (MT039446.1) and putative mutant strain (NA-cys3) *B. paralicheniformis* under SSF; Temperature 37 °C, press mud as substrate 40 g, substrate to diluent ratio 1:1, inoculum size 5% (v/w), glucose conc. 5% (w/v); Kinetic parameters: Specific rate constant for biomass formation q_x (µg/L/h), specific rate constant for substrate consumption q_s (µg/L/h)

The q_x kept decreasing after that to 0.094 µg/L/h at 72 h. The same trend was observed for NA-cys3. Similarly, the q_s decreased between 12 and 36 h, remaining almost constant from 24 to 36 h. After 36 h, a sudden increase in q_s was observed from 0.517 µg/L/h at 36 h to 0.069 µg/L/h at 48 h for the putative mutant strain. A sudden decrease in q_s was observed after 48 h until 72 h (0.135 µg/L/h for MT039446.1 and 0.069 µg/L/h for NA-cys3).

The same trend was shown by wild-type (MT039446.1) *B. paralicheniformis* under SSF. The dynamics of the particular rate constants of the biomass synthesis (q_x) and substrate utilization (q_s) in *B. paralicheniformis* during SSF showed significant kinetic

deviation between the wild-type (MT039446.1) and the putative mutant strain (NA-cys3) and, as a result, the efficiency of acetoin biosynthesis. There was an initial increase in q_x followed by a gradual decrease seen in both strains, implying that there was active biomass accumulation during the early growth stages. This approach of the exponential growth phase is supported by findings of Chen *et al.* (2020). This trend could be linked to microbial growth kinetics as maximum q_x corresponds to high cell growth until nutrients are limiting and result in low growth rates as demonstrated by Zhang *et al.* (2019).

The NA-cys3 strain exhibited a sudden mid-phase surge in q_s, possibly as a sign of a metabolic adaptation or stress response that temporarily boosted the uptake of substrates. Then it decreased towards the end of the phase-again consistent with *Bacillus subtilis* fermentations where the rate of substrate uptake varies in response to oxygen or nutrient limitation as reported by Liu *et al.* (2021). This type of kinetics could be compare to publish literature data by Zhao *et al.* (2022) on acetoin producing *Bacillus* spp., where q_s tends to decline following peak growth because of the shifting of carbon metabolism toward the synthesis of secondary metabolites. These findings suggest that further industrialization of SSF is possible by optimizing parameters used, especially in the shift between the exponential and stationary phases, to increase metabolic activity and yield.

Overall Comparison of Parameters for Specific Acetoin Activity

The fermentation performance and acetoin production were compared at different incubation time points to evaluate changes over the course of the fermentation process. Table 1 illustrates that NA-cys3 mutant had a visible advantage in productivity in comparison with the wild-type in the context of all measurement time points. The mutant exhibited an increased rate of building up of protein soluble and acetoin especially at the middle stage of 12 to 48 h, which indicates an ability of the mutant to have increased capacity in both primary (protein synthesis) and secondary (acetoin) metabolism at mid-fermentation phase. This observation was consistent with findings in stress-adapted *Bacillus* strains, showing that selective pressure led to the upregulating of the acetoin pathway and increased catalytic activity of enzyme-related genes such as 1-acetolactate synthase and decarboxylase (Li *et al.* 2021). Activity decreased in both strains after 48 h of growth probably as a result of nutrient exhaustion, pH shifts, and potential feedback inhibition of product accumulated products that were documented in stationary-phase *Bacillus* fermentations (Sun *et al.* 2023). The larger absolute values of NA-cys3 at all times indicate that mutation possibly added persisting metabolic preferences towards acetoin despite poor late-phase conditions. Of particular interest, the maximum specific activities in NA-cys3 were more than twice those of the wild-type, further supporting the idea that strain optimization aimed at optimizing biocatalytic activity need not decrease overall protein production.

Table 1. Overall Comparison of Kinetic Parameters for Enhanced Acetoin Production by Wild-type (MT039446.1) and Putative Mutant Strain (NA-cys3) *B. paralicheniformis* Under SSF*

Time of Incubation (h)	Protein Content (µg/mL)		Acetoin Production (mg/mL)		Specific Acetoin Activity (mg/mL)	
	MT039446.1	NA-cys3	MT039446.1	NA-cys3	MT039446.1	NA-cys3
12	46.0 ± 2.3	35.0 ± 1.7	2.92 ± 0.146	8.98 ± 0.449	8.98	134
24	69.0 ± 3.4	72.0 ± 3.6	8.35 ± 0.417	14.75 ± 0.738	14.75	576
36	122.0 ± 6.1	159.0 ± 7.9	11.74 ± 0.587	19.06 ± 0.953	19.06	1432
48	198.0 ± 9.9	264.0 ± 13.2	12.99 ± 0.65	24.97 ± 1.248	24.97	2572
60	209.0 ± 10.4	288.0 ± 14.4	9.55 ± 0.478	17.68 ± 0.884	17.68	1995
72	213.0 ± 10.6	294.0 ± 14.7	6.83 ± 0.342	4.875 ± 0.244	4.875	1454

*Temperature 37 °C, press mud as substrate 40 g, substrate to diluent ratio 1:1, inoculum size 5% (v/w), glucose conc. 5% (w/v), incubation time 48 h;
± Indicates standard deviation (± sd set at 5%) amongst the values of three parallel replicates. The sum mean values differ significantly at $p \leq 0.05$ from each other in one set, under one way ANOVA.

Overall Fermentative Optimals for Enhanced Acetoin Production

The overall performance indicators in optimized SSF media, as shown in Table 2, indicate that the NA-cys3 mutant had a better result than the wild-type in all production-related aspects. Final cell density was higher (as reflected by nearly doubled turbidity readings), and the property of substrate assimilation was also improved (as shown by an increase of glucose consumption). The enhanced protein level and dry cell weight also proved the vigorous cell growth and together with elevated product yield indicated the effective connections between main and secondary metabolism. A similar positive relationship between increased dry biomass and product yield has been reported in genetically improved *E. coli* strains that share deregulated upstream biosynthetic pathways to increased growth and biosynthesis of the target metabolite. The high rate of glucose uptake observed in NA-cys3 might be due to upregulated transporters and/or better glycolysis flux that could supplement pyruvate availability to the generation of acetoin. In comparison, the low uptake substrate in the wild-type restricts the flow of carbon in acetoin pathway leading to smaller yields. This metabolic landscape showed that the metabolism of NA-cys3 can support high levels of biomass productivity and improved product specificity, thus qualifying it as an improved production strain in the given SSF parameters. Optimizing both growth and yield is a positive aspect in batch SSF because the length of the process and efficiency of feedstocks directly affect scalability and cost-efficiency. The successful utilization of press mud as the fermentation substrate further demonstrates the feasibility of converting an abundant agro-industrial residue into a value-added biochemical. This observation is consistent with previous reports highlighting that nutrient-rich agro-industrial by-products can effectively support microbial fermentation while reducing production costs and promoting sustainable biomass valorization (Pandey *et al.* 2000; Solomon 2016).

Table 2. Overall Fermentative Optimals for Enhanced Acetoin Production by Wild-type (MT039446.1) and Putative Mutant Strain (NA-cys3) *B. paralicheniformis* Under SSF*

Variants	MT039446.1	NA-cys3
Turbidity	0.82 ± 0.032	1.68 ± 0.087
Glucose consumption (mg/mL)	28.0 ± 1.4	43.0 ± 2.15
Acetoin production (mg/mL)	12.99 ± 0.65	24.97 ± 1.248
Protein content (µg/mL)	198.0 ± 9.9	264.0 ± 13.2
Dry cell weight (µg/mL)	15.0 ± 0.75	18.0 ± 0.9

*Temperature 37 °C, press mud as substrate 40 g, substrate to diluent ratio 1:1, inoculum size 5% (v/w), glucose conc. 5% (w/v), incubation time 48 h;
± Indicates standard deviation (± sd set at 5%) amongst the values of three parallel replicates. The sum mean values differ significantly at $p \leq 0.05$ from each other in one set, under one way ANOVA.

Limitation

A limitation of the present study is that chromatographic confirmation of acetoin by HPLC or GC–MS was not performed. Future studies will incorporate these analytical techniques to provide definitive identification and accurate quantification of the fermentation product.

CONCLUSIONS

1. This study demonstrated a sustainable and cost-effective approach for acetoin production using *Bacillus paralicheniformis* under solid-state fermentation (SSF), employing press mud as the primary carbon source.
2. Process optimization, particularly through controlled variation of incubation time, significantly improved acetoin yield.
3. Product identification was confirmed using UV–visible spectroscopy and Fourier transform infrared (FTIR) analysis, while scanning electron microscopy (SEM), and X-ray diffraction (XRD) revealed substantial morphological and structural changes in the substrate during fermentation.
4. Kinetic evaluation provided detailed insights into microbial growth, substrate utilization, and product formation for both strains, supporting the feasibility of process scale-up and enhanced production efficiency.
5. Overall, the findings establish *B. paralicheniformis* as a promising candidate for acetoin biosynthesis and highlight the potential of converting agro-industrial waste into high-value biochemicals.
6. This work demonstrates the potential of agro-industrial waste valorization as a sustainable approach for industrial biotechnology and aligns with the principles of the circular bioeconomy.

7. Future research should focus on scaling up the fermentation process in pilot- and industrial-scale bioreactors, evaluating process economics, and integrating downstream purification strategies. In addition, metabolic engineering and omics-based analyses of the mutant strain could provide insights into the molecular mechanisms underlying enhanced acetoin production and further improve process efficiency.

ACKNOWLEDEGMENTS

The authors wish to thank Mohsin Hayyat, Department of Chemistry, Government College University, Lahore and Mr. Farrukh Ahmad from University of Engineering and Technology, Lahore for their cooperation in the characterization work. The authors express their gratitude to Princess Nourah bint Abdulrahman University Researchers Supporting Project number (PNURSP2026R924), Princess Nourah bint Abdulrahman University, Riyadh, Saudi Arabia

Competing Interests

The authors declare that there are no conflicts of interest.

Availability of Data and Material

All the data generated in this research work have been included in this manuscript.

REFERENCES CITED

Afshar, P. G., Honarvar, M., Gharachorloo, M., Eshratabadi, P., and Bazyar, B. (2014). "Investigation of the physico-chemical properties of press mud: A sugar industry waste," *Adv. Environ. Biol.* 8(13), 1053-1058.

Afzal, F., Ali, S., Ahmad, M. U., Awan, M. U. F., Khan, A. A., Al-Hoshani, N., Mohamed, R. A. E. H., Alrayyani, M. A., Alsaggaf, W. T., Sagini, H. A., Alwabsi, H. A., and Elkhadragy, M. F. (2026). "Investigating superior environmental microfluidic carbon sequestration using *Hydnum repandum*-mediated ZnO-nanoconjugates," *Open Chem.* 24(1), article 20250248. https://doi.org/10.1515/chem-2025-0248

Andrews, G. F. (1993). "The yield equations in the modeling and control of bioprocesses," *Biotechnol. Bioeng.* 42(5), 549-556. https://doi.org/10.1002/bit.260420502

Bae, S. J., Kim, S., and Hahn, J. S. (2016). "Efficient production of acetoin in *Saccharomyces cerevisiae* by disruption of 2,3-butanediol dehydrogenase and expression of NADH oxidase," *Sci. Rep.* 6(1), article 27667. https://doi.org/10.1038/srep27667

Bentley, W. E., Mirjalili, N., Andersen, D. C., Davis, R. H., and Kompala, D. S. (1990). "Plasmid-encoded protein: The principal factor in the 'metabolic burden' associated with recombinant bacteria," *Biotechnol. Bioeng.* 35(7), 668-681. https://doi.org/10.1002/bit.260350704

Bibra, M., Kunreddy, V. R., and Sani, R. K. (2018). "Thermostable xylanase production by *Geobacillus* sp. strain DUSELR13, and its application in ethanol production with lignocellulosic biomass," *Microorganisms* 6(3), article 93. https://doi.org/10.3390/microorganisms6030093

Chandel, A. K., Garlapati, V. K., Singh, A. K., Antunes, F. A. F., and da Silva, S. S. (2018). "The path forward for lignocellulose biorefineries: Bottlenecks, solutions, and perspective on commercialization," *Bioresour. Technol.* 264, 370-381. https://doi.org/10.1016/j.biortech.2018.06.004

Cole, S., Ellis, M., Sowards, J., and McCunn, L. R. (2017). "Pyrolysis and matrix-isolation FTIR of acetoin," in: *72nd International Symposium on Molecular Spectroscopy*, Paper WE01, Champaign-Urbana, IL, USA. https://doi.org/10.15278/isms.2017.WE01

Dotaniya, M. L., Datta, S. C., Biswas, D. R., Dotaniya, C. K., Meena, B. L., Rajendiran, S., Regar, K. L., and Lata, M. (2016). "Use of sugarcane industrial by-products for improving soil health and crop productivity: A review," *Int. J. Recycl. Org. Waste Agric.* 5, 185-194. https://doi.org/10.1007/s40093-016-0132-8

Eid, M. M. (2022). "Characterization of nanoparticles by FTIR and FTIR-microscopy," in: *Handbook of Consumer Nanoproducts*, Springer, Singapore, pp. 1-30. https://doi.org/10.1007/978-981-15-6453-6_89-1

Fatimah, S., Ragadhita, R., Al Husaeni, D. F., and Nandiyanto, A. B. D. (2022). "How to calculate crystallite size from X-ray diffraction (XRD) using Scherrer method," *ASEAN J. Sci. Eng.* 2(1), 65-76. https://doi.org/10.17509/ajse.v2i1.37647

Gong, Z., Zhang, S., and Liu, J. (2023). "Recent advances in chitin biosynthesis associated with the morphology and secondary metabolite synthesis of filamentous fungi in submerged fermentation," *J. Fungi* 9(2), article 205. https://doi.org/10.3390/jof9020205

Gui, G., Liu, H., and Zhang, X. (2020). "Metabolic engineering of *Bacillus licheniformis* for production of acetoin," *Front. Bioeng. Biotechnol.* 8, article 125. https://doi.org/10.3389/fbioe.2020.00125

Gumanta, F. S., Ghadr, S., Chen, C. S., Liu, C. H., Hung, C., and Assadi-Langroudi, A. (2023). "Enhancing the mechanical and hydromechanical behaviors of mudstone soils using sugarcane press mud," *Transp. Geotech.* 40, article 100948. https://doi.org/10.1016/j.trgeo.2023.100948

Gupta, N., Tripathi, S., and Balomajumder, C. (2011). "Characterization of pressmud: A sugar industry waste," *Fuel* 90(1), 389-394. https://doi.org/10.1016/j.fuel.2010.08.021

Jha, D., Kusne, A. G., Al-Bahrani, R., Nguyen, N., Liao, W. K., Choudhary, A., and Agrawal, A. (2019). "Peak area detection network for directly learning phase regions from raw X-ray diffraction patterns," in: *2019 International Joint Conference on Neural Networks (IJCNN)*, IEEE, p. 1-8.

Ji, X. J., Huang, H., and Ouyang, P. K. (2011). "Microbial 2,3-butanediol production: A state-of-the-art review," *Biotechnol. Adv.* 29(3), 351-364. https://doi.org/10.1016/j.biotechadv.2011.01.007

Jia, X., Peng, X., Liu, Y., and Han, Y. (2017). "Conversion of cellulose and hemicellulose of biomass simultaneously to acetoin by thermophilic simultaneous saccharification and fermentation," *Biotechnol. Biofuels* 10, article 232. https://doi.org/10.1186/s13068-017-0924-8

Kartika, A. A., Sunarharum, W. B., Asli, N. A., Tan, E. T. T., Rusop, M., Mahatmanto, T., Prananto, Y. P., Shuhairi, D. N. M., and Malek, N. S. A. (2026). "Enhancing the functional quality of Liberica nano-coffee *via* yeast-lactic fermentation and nano-milling techniques," *Trends Sci.* 23(1), article 11008. https://doi.org/10.48048/tis.2026.11008

Khan, H., Yerramilli, A. S., D'Oliveira, A., Alford, T. L., Boffito, D. C., and Patience, G. S. (2020). "Experimental methods in chemical engineering: X-ray diffraction spectroscopy (XRD)," *Can. J. Chem. Eng.* 98(6), 1255-1266. https://doi.org/10.1002/cjce.23747

Lawford, H. G., and Rousseau, J. D. (1993). "Mannose fermentation by ethanologenic recombinants of *Escherichia coli* and kinetical aspects," *Biotechnol. Lett.* 15, 615-620.

Lee, J. H., Lee, D. Y., Lee, S. K., Kim, H. R., Chun, Y., Yoo, H. Y., Kwak, H. S., Park, C., Lee, J. H., and Kim, S. W. (2021). "Development of 2,3-butanediol production process from *Klebsiella aerogenes* ATCC 29007 using extracted sugars of *Chlorella pyrenoidosa* and biodiesel-derived crude glycerol," *Processes* 9(3), article 517. https://doi.org/10.3390/pr9030517

Lee, S. Y., Papoutsakis, E. T., and Bailey, J. E. (1999). "Substrate uptake and utilization kinetics in batch cultures of *Escherichia coli* with reduced pyruvate dehydrogenase activity," *Biotechnol. Bioeng.* 44(5), 1181-1190. https://doi.org/10.1002/bit.260440912

Li, S., Gao, X., Xu, N., Liu, L., and Chen, J. (2014). "Enhancement of acetoin production in *Candida glabrata* by in silico-aided metabolic engineering," *Microb. Cell Fact.* 13, article 55. https://doi.org/10.1186/1475-2859-13-55

Liu, Z., Chen, J., and Huang, L. (2021). "Substrate utilization dynamics in *Bacillus subtilis* fermentation: Impact on metabolite yields," *J. Biotechnol.* 325, 34-41. https://doi.org/10.1016/j.jbiotec.2020.12.004

Mao, Y., Fu, J., Tao, R., Huang, C., Wang, Z., Tang, Y. J., Chen, T., and Zhao, X. (2017). "Systematic metabolic engineering of *Corynebacterium glutamicum* for the industrial-level production of optically pure D-(-)-acetoin," *Green Chem.* 19(23), 5691-5702. https://doi.org/10.1039/C7GC02753B

Mourdikoudis, S., Pallares, R., and Thanh, N. T. K. (2018). "Characterization techniques for nanoparticles: Comparison and complementarity upon studying nanoparticle properties," *Nanoscale* 10(3), 12871-12934. https://doi.org/10.1039/C8NR02278J

Nandiyanto, A. B. D., Oktiani, R., and Ragadhita, R. (2019). "How to read and interpret FTIR spectroscope of organic material," *Indones. J. Sci. Technol.* 4(1), 97-118.

Nielsen, J. (1999). "Fermentation kinetics," in: *Fermentation Microbiology and Biotechnology*, Taylor & Francis, Boca Raton, FL, USA, pp. 69-120.

Nimbalkar, P. R., Khedkar, M. A., Gaikwad, S. G., Chavan, P. V., and Bankar, S. B. (2017). "New insight into sugarcane industry waste utilization (press mud) for cleaner biobutanol production by using *Clostridium acetobutylicum* NRRL B-527," *Appl. Biochem. Biotechnol.* 183(3), 1008-1025. https://doi.org/10.1007/s12010-017-2479-3

Pandey, A., Soccol, C. R., Nigam, P., and Soccol, V. T. (2000). "Biotechnological potential of agro-industrial residues. I: Sugarcane bagasse," *Bioresour. Technol.* 74(1), 69-80. https://doi.org/10.1016/S0960-8524(99)00142-X

Picollo, M., Aceto, M., and Vitorino, T. (2019). "UV-Vis spectroscopy," *Phys. Sci. Rev.* 4(4), article 20180008. https://doi.org/10.1515/psr-2018-0008

Pirt, S. J. (1975). *Principles of Microbe and Cell Cultivation*, Blackwell Scientific Publications, London, UK, pp. 16, 53-67, 114.

Relucenti, M., Familiari, G., Donfrancesco, O., Taurino, M., Li, X., Chen, R., Artini, M., Papa, R., and Selan, L. (2021). "Microscopy methods for biofilm imaging: Focus on SEM and VP-SEM pros and cons," *Biology* 10(1), article 51. https://doi.org/10.3390/biology10010051

Saini, M., Anu, Rapoport, A., Tiwari, S. K., Singh, D., Malik, V., Kumar, S., and Singh, B. (2023). "Bioacetoin production by *Bacillus subtilis* subsp. *subtilis* using enzymatic hydrolysate of lignocellulosic biomass," *Fermentation* 9(8), article 698. https://doi.org/10.3390/fermentation9080698

Sharma, R., Garg, P., Kumar, P., Bhatia, S. K., and Kulshrestha, S. (2020). "Microbial fermentation and its role in quality improvement of fermented foods," *Fermentation* 6(4), article 106. https://doi.org/10.3390/fermentation6040106

Singh, R. S., Chauhan, K., and Jindal, A. (2018). "Response surface optimization of solid-state fermentation for inulinase production from *Penicillium oxalicum* using corn bran," *J. Food Sci. Technol.* 55, 2533-2540. https://doi.org/10.1007/s13197-018-3173-3

Singh, S., Gade, J. V., Verma, D. K., Elyor, B., and Jain, B. (2024). "Exploring ZnO nanoparticles: UV-visible analysis and different size estimation methods," *Opt. Mater.* 152, article 115422. https://doi.org/10.1016/j.optmat.2024.115422

Sivagurunathan, P., Sahoo, P. C., Kumar, M., Gupta, R. P., Srivastava, U., and Sharma, A. (2026). "Iron oxide nanoparticle augmented yeast biohybrid for enhanced ethanol fermentation *via* metabolic and electron transfer modulation," *Bioresource Technol. Rep.* 25, article 102643. https://doi.org/10.1016/j.biteb.2026.102643

Śliżewska, K., and Chlebicz-Wójcik, A. (2020). "Growth kinetics of probiotic *Lactobacillus* strains in the alternative, cost-efficient semi-solid fermentation medium," *Biology* 9(12), article 423. https://doi.org/10.3390/biology9120423

Snedecor, G. W., and Cochran, W. G. (1980). *Statistical Methods*, 7th Ed., Iowa State University Press, Ames, IA, USA.

Solomon, S. (2016). "Sugarcane by-products based industries in India," *Sugar Tech.* 18(3), 230-245. https://doi.org/10.1007/s12355-016-0459-6

Thakar, M. A., Jha, S., Phasinam, K., Manne, R., Qureshi, Y., and Hari Babu, V. V. (2022). "X-ray diffraction (XRD) analysis and evaluation of antioxidant activity of copper oxide nanoparticles synthesized from leaf extract of *Cissus vitiginea*," *Mater. Today Proc.* 51, 319-324. https://doi.org/10.1016/j.matpr.2021.05.410

Tian, Y., Xu, H., Liu, J., Chen, W., Sun, W., and Chen, Y. (2016). "Construction of acetoin high-producing *Bacillus subtilis* strain," *Biotechnol. Biotechnol. Equip.* 30(4), 700-705. https://doi.org/10.1080/13102818.2016.1179592

Ural, N. (2021). "The significance of scanning electron microscopy (SEM) analysis on the microstructure of improved clay: An overview," *Open Geosci.* 13(1), 197-218. https://doi.org/10.1515/geo-2020-0145

Vogt, C., Wondergem, C. S., and Weckhuysen, B. M. (2023). "Ultraviolet-visible (UV-Vis) spectroscopy," in: *Springer Handbook of Advanced Catalyst Characterization*, Springer International Publishing, Cham, Switzerland, pp. 237-264. https://doi.org/10.1007/978-3-031-07125-6_11

Wang, Q., Bao, T., Hu, M., Xu, M., Rao, Z., and Zhang, X. (2025). "Efficient acetoin production in *Bacillus subtilis* by multivariate modular metabolic engineering with spatiotemporal modulation," *ACS Sustainable Chem. Eng.* 13(5), 1927-1936. https://doi.org/10.1021/acssuschemeng.4c06511

Welden, M., Severins, R., Poghossian, A., Wege, C., Bongaerts, J., Siegert, P., Keusgen, M., and Schöning, M. J. (2022). "Detection of acetoin and diacetyl by a tobacco mosaic virus-assisted field-effect biosensor," *Chemosensors* 10(6), article 218. https://doi.org/10.3390/chemosensors10060218

Xiao, Z., and Lu, J. (2014). "Strategies for enhancing fermentative production of acetoin: A review," *Biotechnol. Adv.* 32, 492-503. https://doi.org/10.1016/j.biotechadv.2014.01.002

Xiao, Z., and Lu, J. R. (2014). "Generation of acetoin and its derivatives in foods," *J. Agric. Food Chem.* 62, 6487-6497. https://doi.org/10.1021/jf5013902

Xu, H., Tian, Y., Wang, S., Zhu, K., Zhu, L., He, Q., Li, W., and Liu, J. (2021). "Batch fermentation kinetics of acetoin produced by *Bacillus subtilis* HB-32," *Prep. Biochem. Biotechnol.* 51(10), 1004-1007. https://doi.org/10.1080/10826068.2021.1885047

Xu, H., Tian, Y., Zhu, K., Wang, S., Zhu, L., He, Q., Li, W., and Liu, J. (2022). "A new quantitative determination method of acetoin," *Int. J. Curr. Microbiol. Appl. Sci.* 11(3), 80-85. https://doi.org/10.20546/ijcmas.2022.1103.010

Yafetto, L. (2022). "Application of solid-state fermentation by microbial biotechnology for bioprocessing of agro-industrial wastes from 1970 to 2020: A review and bibliometric analysis," *Heliyon* 8(3), article e09173.

Yang, S., Mohagheghi, A., Franden, M. A., Chou, Y. C., Chen, X., Dowe, N., Himmel, M. E., and Zhang, M. (2016). "Metabolic engineering of *Zymomonas mobilis* for 2,3-butanediol production from lignocellulosic biomass sugars," *Biotechnol. Biofuels* 9(1), article 189. https://doi.org/10.1186/s13068-016-0606-y

Yang, T., Rao, Z., Zhang, X., Xu, M., Xu, Z., and Yang, S. (2017). "Metabolic engineering strategies for acetoin and 2,3-butanediol production: Advances and prospects," *Crit. Rev. Biotechnol.* 37, 990-1005. https://doi.org/10.1080/07388551.2017.1299680

Zhang, J., Li, X., and Zhou, Y. (2019). "Modelling microbial kinetics in solid-state fermentation for industrial applications," *Biochem. Eng. J.* 144, 120-129. https://doi.org/10.1016/j.bej.2019.01.009

Zhao, H., Sun, J., and Li, W. (2022). "Acetoin production from renewable substrates using *Bacillus* spp.: Metabolic pathways and fermentation strategies," *Front. Bioeng. Biotechnol.* 10, article 832845. https://doi.org/10.3389/fbioe.2022.00832

Zhu, C., Shen, T., Liu, D., Wu, J., Chen, Y., Wang, L., Guo, K., Ying, H., and Ouyang, P. (2016). "Production of liquid hydrocarbon fuels with acetoin and platform molecules derived from lignocellulose," *Green Chem.* 18(7), 2165-2174. https://doi.org/10.1039/C5GC02414E

Article submitted: June 27, 2026; Peer review completed: July 25, 2026; Revised version received: August 7, 2026; Accepted: August 9, 2026; Published: August 24, 2026.
DOI: 10.15376/biores.21.4.9962-9984